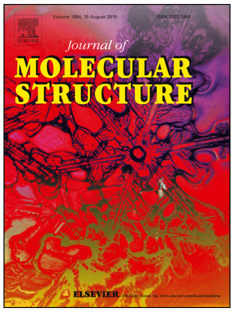

Crystal structures and thermal behaviour of double complex compounds incorporating the $[Cr\{CO(NH_2)_2\}_6]^{3+}$ cation

S.I. Pechenyuk, A.A. Zolotarev, A.N. Gosteva, D.P. Domonov, A.A. Shimkin

PII: S0022-2860(17)30880-3
DOI: 10.1016/j.molstruc.2017.06.099
Reference: MOLSTR 23985

To appear in: *Journal of Molecular Structure*

Received Date: 30 March 2017
Revised Date: 20 June 2017
Accepted Date: 20 June 2017

Please cite this article as: S.I. Pechenyuk, A.A. Zolotarev, A.N. Gosteva, D.P. Domonov, A.A. Shimkin, Crystal structures and thermal behaviour of double complex compounds incorporating the $[Cr\{CO(NH_2)_2\}_6]^{3+}$ cation, *Journal of Molecular Structure* (2017), doi: 10.1016/j.molstruc.2017.06.099.

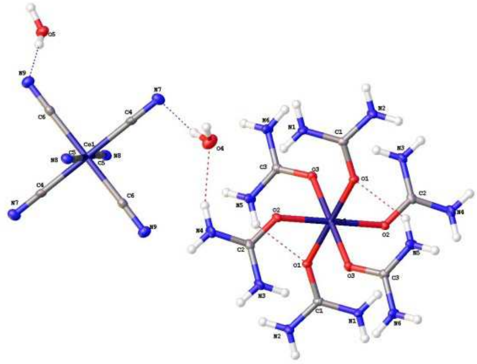
O5
N9
N7
C6
C4
Co1
N8
C5
C5
N8
C4
C6
N7
N9
O4
N6
N1
C1
N2
N3
C3
O3
O1
C2
N5
N4
O2
O2
N6
N4
C2
O1
O3
N5
C3
N3
C1
N1
N6
N2

Crystal structures and thermal behaviour of double complex compounds incorporating the $[Cr\{CO(NH_2)_2\}_6]^{3+}$ cation

Pechenyuk S.I.[a], Zolotarev A.A.[b], Gosteva A.N.[a], Domonov D.P.[a,*], Shimkin A.A.[c]
[a]*I.V.Tananaev Institute of Chemistry and Technology of Rare Elements and Mineral Raw Materials of the Kola Science Center, RAS, Akademgorodok 26a, Apatity, Russian*
[b]*Saint Petersburg State University, Saint Petersburg, Russian*
[c]*All-Russia Research Institute of Aircraft Materials, Moscow, Russian*

* Corresponding author.

Abstract. Double complex compounds (DCC) of the $[Cr(ur)_6][Fe(CN)_6]\cdot 4H_2O$ (**I**), $[Cr(ur)_6][Co(CN)_6]\cdot 4H_2O$ (**II**), $[Cr(ur)_6][Fe(Ox)_3]\cdot 2H_2O$ (**III**), and $[Cr(ur)_6][Co(Ox)_3]\cdot 3.5H_2O$ (**IV**) composition, where *ur* is $CO(NH_2)_2$, *Ox* – $C_2O_4^{2-}$ have been synthesized and their crystal structures have been studied. The DCC **I**, **II** and **IV** are triclinic (P-1); **III** is orthorhombic ($C222_1$). The DCC thermal behavior in air and argon atmospheres was analyzed by the following parameters: the temperature interval of total decomposition and the nature of gaseous and solid products. The end solid products in air were FeO and $FeCr_2O_4$ for **I**, a mixture of $CoCr_2O_4$ + Co_2CrO_4 for **II** and **IV** and an X-ray amorphous phase with composition $CrFeO_{2.5}$ for **III**. The gaseous products were HCN, NH_3, HNCO, N_2O, CO, CO_2, N_2, and urea. The temperatures of total decomposition in air were: **I**, **II** 400°C, **III** – 350°C, **IV** – 460°C. In argon, the solid residue contained, besides the oxides, 7-30% of carbon up to 1000°C.

Key words: double complex compound, thermolysis, crystal structure, X-ray diffraction, IR spectroscopy

1. Introduction

Thermal decomposition of various complex compounds is now recognized as a promising technique in the production of composite materials of which many are unobtainable otherwise. An example of such composites are metastable bimetallic or metal-carbon systems. One of the best precursors in the synthesis of these composites are double or heteronuclear complex compounds (DCC). We have investigated the DCC of the $[M_1L_a]_x[M_2X_b]_y$ type, where M_1 and M_2 are metals, L are neutral ligands, and X are acidoligands, as precursors for the synthesis of bimetallic materials [1]. Thermolysis is a process which allows to remove the ligands from DCC by way of careful heating. Thermolysis in general is represents a complex solid-phase process involving redox and substitution reactions both within the solid phase and at the interfaces, and the formation of new solid phases and interfaces. The formation of new solid phases is attended by either the formation of a porous structure or residue crystallization and releasing of gaseous products from the solid phases. The purposeful synthesis of a certain product requires information about all thermolysis stages. Thus, it is important to know the crystalline structure of initial and intermediate products because both the formation of new solid phases and gas release are related to the movement (diffusion) of atoms within the solid phase and across the interfaces.

Complexes containing the $[Cr\{CO(NH_2)_2\}_6]^{3+}$ ($CO(NH_2)_2$ – urea) cation and $[M(CN)_6]^{3-}$ and $[M(C_2O_4)_3]^{3-}$ anions have been known for a long time [2] but, to our knowledge, there is no evidence on their crystal structure and thermal behavior. Interestingly, the thermal decomposition of these DCC produces highly dispersed chromospinel, pseudochromite and mixed oxides.

The aim of this work is to study the crystal structures, characterize the properties, and perform a comparative analysis of the thermal decomposition procedure of DCC $[Cr(ur)_6][Fe(CN)_6]\cdot 4H_2O$ (**I**), $[Cr(ur)_6][Co(CN)_6]\cdot 4H_2O$ (**II**), $[Cr(ur)_6][Fe(Ox)_3]\cdot 2H_2O$ (**III**), $[Cr(ur)_6][Co(Ox)_3]\cdot 3.5H_2O$ (**IV**), including the nature of resulting solid and gaseous products.

2. Experimental

2.1. Synthesis

DCC **I-II** were synthesized from hexaureachromium(III)–chloride $[Cr(ur)_6]Cl_3\cdot 3H_2O$ obtained according to [3] by means of mixing a water solution with an equivalent quantity of a cation complex and commercial potassium hexacyanoferrate or hexacyanocobaltate (chemically pure), and DCC **III-IV** by means of mixing a solution of the same cation complex with potassium (tris)oxalatoferrate or (tris)oxalatocobaltate obtained according to [3]. For example, 11.45 g (0.02 mol) $[Cr(ur)_6]Cl_3\cdot 3H_2O$ and 6.58 g (0.02 mol) $K_3[Fe(CN)_6]$ were dissolved in a minimal volume of water and blended. This resulted in immediate precipitation of bright-green lamellar crystals, which were filtered and washed with water and ethanol, then dried in a desiccator over alkaline pellets. The yield of **I** was 12.85 g, or 95% of the theoretical value; for **II**, **III** and **IV** it was 98, 99, and 63%, respectively. Complex **IV** is probably more soluble in comparison to 3 other compounds.

2.2. Physical measurements

The DCC were characterized using the XRD, IR spectroscopy. Metals in the DCC were analyzed using an AAnalyst 400 spectrometer in DCC solutions in *aqua regis*. Analysis for carbon contents was performed at an ELTRA CS-2000 automatic analyzer (Table 1). The powder XRD analysis of the DCC was performed using a Shimadzu XRD 6000 diffractometer (CuK_α radiation, graphite monochromator). The powder diffraction patterns of the synthesis products correlated with theoretical patterns calculated from the structural data, also revealing monophasity of the products obtained.(Supplementary)

The IR spectra were recorded using a Nicolet 6700 FT-IR spectrometer in the region of 4000-400 cm^{-1} in KBr tablets. The IR spectroscopic studies in the DCC identification were based on [4-6]. IR-spectrum **I** (ν, cm^{-1}): $\nu(OH_2)$ (3440); $\nu(NH_2)$ (3380, 3220); $\nu(C\equiv N)$ (2115); $\delta(OH_2)$ (1640); $\delta(NH_2)$ (1560); $\nu(C\text{-}O)$ (1510); $\rho_w(NH_2)$ (1140); $\nu(C\text{-}N)$ (1040); $\delta(NCO)$ (630); $\delta(NCN)$ (540).

IR-spectrum **II** (ν, cm^{-1}): ν(OH_2) (3450); ν(NH_2) (3350, 3220); ν(C≡N) (2140); δ(OH_2) (1640); δ(NH_2) (1560); ν(C-O) (1500); ρ_w(NH_2) (1140); ν(C-N) (1030); δ(NCO) (760); δ(NCN) (530); ν(*M*-C) (400).

IR-spectrum **III** (ν, cm^{-1}): ν(OH) (3580); ν(OH_2) (3470); ν(NH_2) (3420, 3210); ν_{as}(C=O) (1680); δ(NH_2) (1560); ν(C-O) (1500); ν_s(C-O)+ ν(C-C) (1370); ν_s(C=O)+ δ(O-C=O) (1260, 1220); ρ_w(NH_2) (1150); ν(C-N) (1020); ν_s(C-O)+ δ(O-C=O) (880); δ(O-C=O)+ ν(*M*-O) (780); δ(NCN) (540).

IR-spectrum **IV** (ν, cm^{-1}): ν(NH_2) free (3463, 3346); ν(NH_2) bound (3232); ν_{as}(C=O) (1708, 1671); δ_{as}(NH_2) (1632); ν(C=O) (1558); ν(C - N) (1500, 1385); ν_δ(C-O) + δ(O-C=O) (1243); ρ_w(NH_2) (1156); ν_s(C-N) (1034); ν_s(C-O) (900); ρ(OH_2) (849); δ(O-C=O) + ν(*M*-O) (822, 804); ω(C-O) (770); ρ(OH_2) (630); ν(*M*-O) + ν(C-C) (559); ν(*M*-O) + δ_{cycl} (444).

2.3. The X-ray structure analyses

The X-ray structure analyses of DCC were conducted at the temperature of 100 K using an Agilent Technologies Excalibur Eos (for **II**, **III**, **IV**) and SuperNova (for **I**) single-crystal diffractometers equipped with a flat CCD detector. The crystallographic data and some refinement parameters of DCC structures are presented in Table 2. The structures were solved by direct methods and refined by means of the SHELX software [7] incorporated in an OLEX2 program complex [8]. The absorption correction was applied in the CrysAlisPro software package [9] empirically, using the spherical harmonics implemented in the SCALE3 ABSPACK scaling algorithm.

Hydrogen atoms were included in the refinement with fixed positional and temperature parameters (in the `riding` model approximation according to the SHELX algorithms), with U_{iso}(H) set to $1.2U_{eq}$(N) and N–H 0.86 Å for NH_2 groups, U_{iso}(H) set to $1.5U_{eq}$(O) and O–H 0.85 Å for H_2O molecules. The CIF files containing the structural information have been deposited in CCDC № 1517429, 1487604, 1487605 and 1487603 for **I, II, III, IV** and are available in the database of organic compound crystal structures at the site *www.ccdc.cam.ac.uk/data_request/cif.*

2.4. *Thermal analyses*

The thermal analyses in air and argon atmospheres were performed using a NETZSCH STA 409 PC/PG device in a covered corundum crucible, with a weight of 6-10 mg and a heating rate of 10 deg/min. The thermographs of the complexes can be seen in Figures 4, 5. For a larger weight (~0.5 g), thermolysis was carried out in a quartz tube reactor inserted into a tube furnace SNOL -02/1250. The IR spectra of gaseous products of thermolysis were analyzed on a Netzsch STA 449 F3 Jupiter simultaneous thermal analyzer combined with a Bruker Tensor 27 FTIR spectrometer. Weighed samples of 17-25 mg was heated in the corundum crucible in a nitrogen atmosphere (99.999%) or synthetic air in a temperature range of 40–1000°C. The heating rate was 10°C min^{-1}. IR spectra were recorded in a range of 550–4000 cm^{-1} with a resolution of 4 cm^{-1} and averaging over 32 scans. The compounds were identified by comparing with the NIST database. The contents of CO and CO_2 were determined using a MAG gas analyzer (”MONITORING”JSC, Saint-Petersburg, Russia). The quantity analysis of the gaseous products of thermolysis (GPT) was performed in the following way: the tube reactor output was supplied with two Drecksel vessels with stripping solutions were sequentially put, the first one containing 0.1M HCl, the second - 0.15 M NaOH + 0.25 M H_2O_2 heated to 80°C. The first solution absorbed ammonia, the second – HCN, HNCO, N_2O with nitrogen oxidation to NO_3^-, which was then determined in the solution (Table 3).

3. Results and discussion

3.1. Description of crystal structures

The DCC **I, II** and **IV** are triclinic (*P*-1); **III** – is orthorhombic (*C*222$_1$) (Table 2). All four DCC structures are described as the structures with isolated anion and cation complexes. The structural units and packing are presented in Figures 1, 2 and 3 by the example of compounds **II, III** and **IV** respectively. The compounds **I** and **II** are isostructural. All central metal ions in the studied DCC have the coordination number 6 and the coordination of chromium, iron and cobalt atoms is represented as almost regular octahedra. The cation octahedron consists of six oxygen atoms of six urea molecules, with average Cr-O bond length equal 1.966 Å. The arrangement of anion include six carbon atoms of six cyano groups, with average bond lengths Fe-C and Co-C equal 1.940 and 1.899 Å for **I** and **II**, respectively, and six oxygen atoms of three oxalate ions with average bond lengths Fe-O and Co-O equal 2.011 Å and 1.897 Å for **III** and **IV** respectively. Figures 1b, 2b and 3b show a packing of complex cations and anions in the structures. As noted before, compounds **I** and **II** are isostructural, with 1 anion and 1 cation per one unit cell between which 4 water molecules (2 crystallographically independent water molecules) are located. One unit cell of compound **III** contains 4 crystallographically equivalent anions, 4 crystallographically equivalent cations and 8 water molecules (1 crystallographically independent water molecule). In the one unit cell of compound **IV** there are 2 crystallographically equivalent anions, 2 crystallographically independent cations and 7 water molecules (3.5 crystallographically independent water molecules). The structural units of the compounds (cations, anions and water molecules) are interconnected by hydrogen and intermolecular bonds (Figures 1, 2, 3). The length of the shortest hydrogen contact D→A for

I is 2.882(4) Å; for **II** - 2.893(3) Å; for **III** - 2.746(4) Å; and for **IV** - 2.783(4) Å. All these structures are based upon isolated anion and cation complexes. The anion and cation octahedra are practically undistorted, that seems characteristic of this DCC type.

3.2. Thermal behavior of DCC

Examination of thermal analysis curves for DCC **I** and **II** in the air atmosphere has revealed that these compounds decompose similarly (Fig. 4a). The outersphere water releases up to ~140°C, which is attended by a small endothermal effect at 100°C. From 120 to 200°C, no mass loss is observed, i.e. the dehydrated complex is stable. Most of the mass is lost between 200 to 400°C as a result of which the residues of calcination correspond to a mixture of $FeO+FeCr_2O_4$ (chromite) for **I** and a mixture $CoCr_2O_4 + Co_2CrO_4$ for **II** [10].

As revealed by qualitative analysis of GPT, there is a connection between the observed effects and the nature of occurring transformations. An example for DCC **I** is presented in Figure 4b. It shows the onset of a simultaneous emission of HCN, NH_3, HNCO and N_2O traces at 175°C continuing until ~400°C. At ~ 250°C, this process is supplemented by the CO_2 emission continuing until ~425°C. According to [11], NH_3 and HNCO are the urea decomposition products and HCN is the product of complex anion decomposition. The HCN emission ends already at 325°C. Since the formation of the main mass of HCN, NH_3 and HNCO is not accompanied by intensive CO_2 emission, the CO_2 is mainly the product of residual ligands oxidation. It is evident that the thermal decomposition of the DCC cation and anion proceeds simultaneously but not sequentially, i.e. anion after cation, as it might be expected from the literature data about the cationic and anionic complexes thermolysis [12-14].

In the cases DCC **II-IV** except on products of urea decomposition, escaping of urea *per se* is sometimes observed. This is confirmed by static experiments including a quantity analysis of GPT at thermolysis of DCC **II** in air (Table 3). A part of urea escapes in a free state (~1 mmol). The content of C in the solid residue is negligibly small. We managed to collect 79% C and 55% N from the total content. Hence it is assumed that a part of C escapes as CO and a part of N - as N_2.

The same similarity of thermal analysis curves for DCC **I** and **II** was observed in inert atmosphere (Fig. 4c). An endothermal effect, attended by outersphere water removal, also emerged in argon and nitrogen atmospheres at 100°C. In argon, as it was in air, achieving of 200°C was marked by a second endoeffect, although latter was greater than in air. Between 200-600°C, there was observed a stepless throw of TG and DSC curves without clear thermal effects. Only at 600-700°C, we recorded a crucial mass loss caused by nitrogen emission detected by analysis of the intermediate products analysis. The composition of GPT in inert atmosphere is qualitatively the same as in air, but the product ratio is different (Fig. 4d). The emissions of HCN, NH_3 and HNCO also begin simultaneously at 200°C, but the temperature range of HCN broadens up to 500°C and the signal intensity of HNCO is greater than that of ammonia. Only traces of CO_2 were obtained. In addition, much of the urea escaped. The residues of calcination of **I** and **II** were found to contain, respectively, Fe_3O_4 (magnetite)+$FeCr_2O_4$ (chromite)+$C_{amorph.}$ and Co + Cr_2O_3+ $CoCrO_4$ (orthorhombic pseudochromite)+ C_{amorph} [10].

These findings correlate with the result of GPT **II** analysis (Table 3). 28% C persist in the solid residue. No CO_2 emission was observed. The other GPT must be urea, CO and N_2.

The thermal behavior of DCC **III** and **IV**, which are similar in composition but not in structure, differs substantially both from each other and from that of **I** and **II**. In air, up to 150 (**III)** and 250°C (**IV**), the TG-DSC curves (Fig. 5a) did not demonstrate any clear effects of outersphere water removal. Beginning with ~160°C, both complexes simultaneously released NH_3 and CO_2 (Fig. 5b). Between 210 and 300°C, CO_2 did not escape. More intensive CO_2 peaks appeared in the range of 300-360 (**III**) and 330–450°C (**IV**) with great exoeffects at 320 and 440°C, respectively. Since the second CO_2 peak was attended by N_2O emission, these effects were attributed to the oxidation of remaining coordinated ligands. The CO_2 emission at around 160°C is the result of partial decomposition of the coordinated oxalate ions because urea does not decompose at this temperature [11]. The products of **III** thermolysis in air did not contain urea, and the gaseous phase analysis indicated CO emission peaks simultaneous with CO_2. The decomposition of **III** and **IV** terminated at 400 and 500°C, respectively. The final products of thermolysis in air were an X-ray amorphous phase with composition $CrFeO_{2.5}$ for **III** and $CoCr_2O_4$ + Co_2CrO_4 for **IV** [10].

Quantitative analysis of GPT **IV** in air has revealed the following (Table 3). Summarily, we managed to collect 98% N and 98% C. The residues of calcination in argon for **III** and **IV** were FeO+$FeCr_2O_4$ (chromite)+$C_{amorph.}$ and Co + Cr_2O_3+ $C_{amorph,}$ respectively.

The thermal analysis curves of DCC **III** and **IV** in argon coincided up to 200 (**III**) and 250°C(**IV**) with appropriate curves observed in air (Fig. 5c). Then decomposition process occurred without clear thermal effects up to 1000°C. CO_2 was emitted in 6 steps. The first step was observed at ~175°C, the next 5 steps were weaker than the first one, and the last effect was observed at 750°C(Fig. 5d). The emission of NH_3 and HNCO began simultaneously with CO_2, but terminated at~400°C. The emission of CO_2 was attended CO for both DCC, the ratio $CO:CO_2 \cong 2:1$, as in the previous paper [15].

Quantitative analysis of GPT **IV** in argon has revealed the following (Table 3). Summarily, we managed to collect 57% N as NH_3 and 23% as HNCO and 23% C as HNCO and 34% as CO_2. 12% C was persisted in the residue of calcination. The remainder C was probably emitted as CO.

4. Conclusion

1. Exploring of the structures and thermal behavior of DCC of the [Cr(*ur)*$_6$][Fe(Co)X_6] type, where X – CN^-, $1/2C_2O_4^{2-}$, has revealed the following. In the first place, it has been established that the isostructural compounds similar in composition behave almost identically, but lead to the formation of different solid products due to different central ions and ligands. Studies of the thermal behavior of DCC **I-IV** afforded to determine the temperature ranges wherein these gaseous products release. 2. It is established that the thermal decomposition of DCC **III** in air at 350°C produces a finely dispersed (X-ray amorphous) phase $CrFeO_{2.5}$. In the other cases the products are crystalline chromites and pseudochromites. 3. DCC **III** with an orthorhombic structure is the least thermally stable. 4. The inner sphere of $[Cr(ur)_6][Co(C_2O_4)_3]$ (**IV**) becomes partly destroyed already at 170°C because of decomposition of one of the coordinated C_2O_4.

References

[1] S.V. Кorenev, A.B. Venedictov, Yu.V. Shubin, S.A. Gromilov, K.V. Yusenko, Journal of Structural Chemistry. 44 (2003) 46-59.

[2] Gmelins Handbuch der anorganische Chemie. 8 Aufl. Chromium. Teil C. 1965, Verlag Chemie GmbH, 32.

[3] G. Brauer, Handbuch der Präparativen Anorganischen Chemie: in Drei Bänden / G. Brauer – Stuttgart: Ferdinand Enke, 1978. – 2113 p.

[4] K. Nakomoto, IR spectra and Raman Spectra of Inorganic and Coordination Compounds. M.: Mir, 1991.

[5] R.B. Penland, S. Mizushima, C. Curran, J.V. Quagliand, J. Amer. Chem. Soc., 79 (1957) 1575-1578.

[6] N. Gorska, E. Mikuli, L. Kotai, Eur. Chem. Bull. 3 (2014) 474-481.

[7] G.M. Sheldrick, Acta Cryst. 64A (2008) 112-122.

[8] O.V. Dolomanov, L.J. Bourhis, R.J. Gildea, J.A.K. Howard, H. Puschmann, J. Appl. Cryst. 42 (2009) 339-341.

[9] CrysAlisPro, Agilent Technologies, Version 1.171.36.20 (release 27-06-2012).

[10] JCPDS-ICDD card. Newtown Square (PA, USA): International Centre for Diffraction Data, 2002.

[11] P.M. Schaber, J. Colson, S. Higgins, J. Brauer, Thermochim. Acta 424 (2004) 131-142.

[12] K.S. Rejitha, S. Mathew, J. Therm. Anal. Calorim. 102 (2010) 931-939.

[13] N. Rajic, D. Stojakovic, R. Gabrovsek J. Therm. Anal. Calorim. 63 (2001) 191-195.

[14] Z. Travnićek, R. Zboril, M.Matikova-Mal’arova, B. Drahoš, J. Černák, Chem.Central Journal. 7 (2013) 28.

[15] S.I. Pechenyuk, Yu.P. Semushina, N.L. Mikhailova, Yu.V. Ivanov, Rus. J. Coord. Chem. 41 (2015) 175-181.

Table 1. Data of elemental and crystal optic analyses of DCC **I-IV**.

DCC	Molecular mass	Contents, wt.%						Crystal habitus
		Cr_{found}	Cr_{calc}	Fe/Co_{found}	Fe/Co_{calc}	C_{found}	C_{calc}	
I	695.8	7.7	7.6	8.1	8.0	21.7	20.7	anisotropic tabular yellow-green crystals
II	699.5	7.5	7.4	8.4	8.4	22.2	20.6	anisotropic light-green tabular crystals
III	768.5	6.6	6.7	7.3	7.3	18.1	18.7	anisotropic tabular crystals, pleochroism on N’p – greyish-blue, on N’g - green
IV	798.4	6.4	6.5	7.6	7.4	17.8	18.0	anisotropic turquoise needle-shapede crystals

Table 2. The crystallographic data and some refinement parameters for structures **I-IV**

DCC	**I**	**II**	**III**	**IV**
Empirical formula	$C_{12}H_{32}N_{18}O_{10}CrFe$	$C_{12}H_{32}N_{18}O_{10}CrCo$	$C_{12}H_{28}N_{12}O_{20}CrFe$	$C_{12}H_{31}N_{12}O_{21.5}CrCo$
Molecular weight	696.40	699.48	768.31	798.42
Crystal system	triclinic	triclinic	orthorhombic	triclinic
Space group	P-1	P-1	$C222_1$	P-1
a (Å)	7.2347(5)	7.2499 (5)	9.0326(6)	11.5268(7)
b (Å)	9.5815(6)	9.5303(7)	21.2902(14)	12.3506(11)
c (Å)	10.4223(7)	10.4286(9)	15.4349(13)	13.3178(8)
α (°)	97.774(5)	97.681(7)	90	96.695(6)
β (°)	91.278(5)	91.850(6)	90	113.644(6)
γ (°)	94.734(5)	94.328(6)	90	114.182(7)
V (Å^3)	712.97(8)	711.39(10)	2968.2(4)	1492.2(3)
Z	1	1	4	2
D_{calc} (g/cm^3)	1.622	1.633	1.719	1.777
μ (mm^{-1})	7.932	1.044	0.958	1.030
F(000)	360.0	361.0	1576.0	820.0
Crystal size(mm^3)	0.25 × 0.19 × 0.11	0.26 × 0.23 × 0.15	0.23 × 0.18 × 0.15	0.28 × 0.24 × 0.15
Radiation	Cu$K\alpha$	Mo$K\alpha$	Mo$K\alpha$	Mo$K\alpha$
Reflexes total/independent	6490/2813	6288/3269	10382/3396	12103/6813
Measuring area 2θ (°)	8.57-144.99	5.44-54.99	5.56-54.99	6.04-55.00
Index range	$-8 \leq h \leq 6$, $-11 \leq K \leq 11$, $-12 \leq l \leq 12$	$-9 \leq h \leq 9$, $-12 \leq k \leq 12$, $-13 \leq l \leq 13$	$-11 \leq h \leq 11$, $-27 \leq k \leq 27$, $-20 \leq l \leq 20$	$-14 \leq h \leq 13$, $-15 \leq k \leq 16$, $-15 \leq l \leq 17$
R_{int}	0.0632	0.0345	0.0534	0.0308
R_1 (I ≥ 2σ(I))	0.0470	0.0356	0.0400	0.0380
wR_2 (I ≥ 2σ(I))	0.1192	0.0845	0.0735	0.0897
R_1 (all data)	0.0544	0.0445	0.0511	0.0495
wR_2 (all data)	0.1275	0.0930	0.0778	0.0988
S	1.031	1.045	1.050	1.028
ρ_{min}, ρ_{max}, e/Å^3	0.70/-0.92	0.34/-0.42	0.41/-0.38	0.56/-0.53
Flack parameter	-	-	-0.014(14)	-

$R_1 = \Sigma||F_o| - |F_c||/\Sigma|F_o|$; $wR_2 = \{\Sigma [w(F_o^2 - F_c^2)^2]/ \Sigma [w(F_o^2)^2]\}^{1/2}$;
$w = 1/[\sigma^2(F_o^2)+(aP)^2 + bP]$, где $P = (F_o^2 + 2F_c^2)/3$; $s = \{\Sigma [w(F_o^2 - F_c^2)]/(n - p)\}^{1/2}$ where n is the number of reflexes and p is the number of refined parameters.

Table 3. The results of quantitative analysis of GTP.

DCC	Atmosphere	Temperature range, °C	Mmol					%*		C in solid residue, %
			DCC	NH_3	N_2O	CO_2	HCN + HNCO or HNCO	N	C	
II	air	20-280	0.77	0.3	-	0.1	1.1	40.3/ 54.6	67.7/ 78.5	<0.01
		280-500		3.2	-	3.9	1.2			
	argon	20-750	0.83	2.4	-	-	1.7	27.5	17.2	28
IV	air	20-300	0.66	1.1	0.3	1.6	-	83.5/ 98	50.6/ 98	<0.1
		300-500		3.0	0,95	4.9	-			
	argon	20-850	0.72	4.9	-	2.9	2.0	80.2	57.0	7

*Nonregistering segregating urea/registering segregated urea

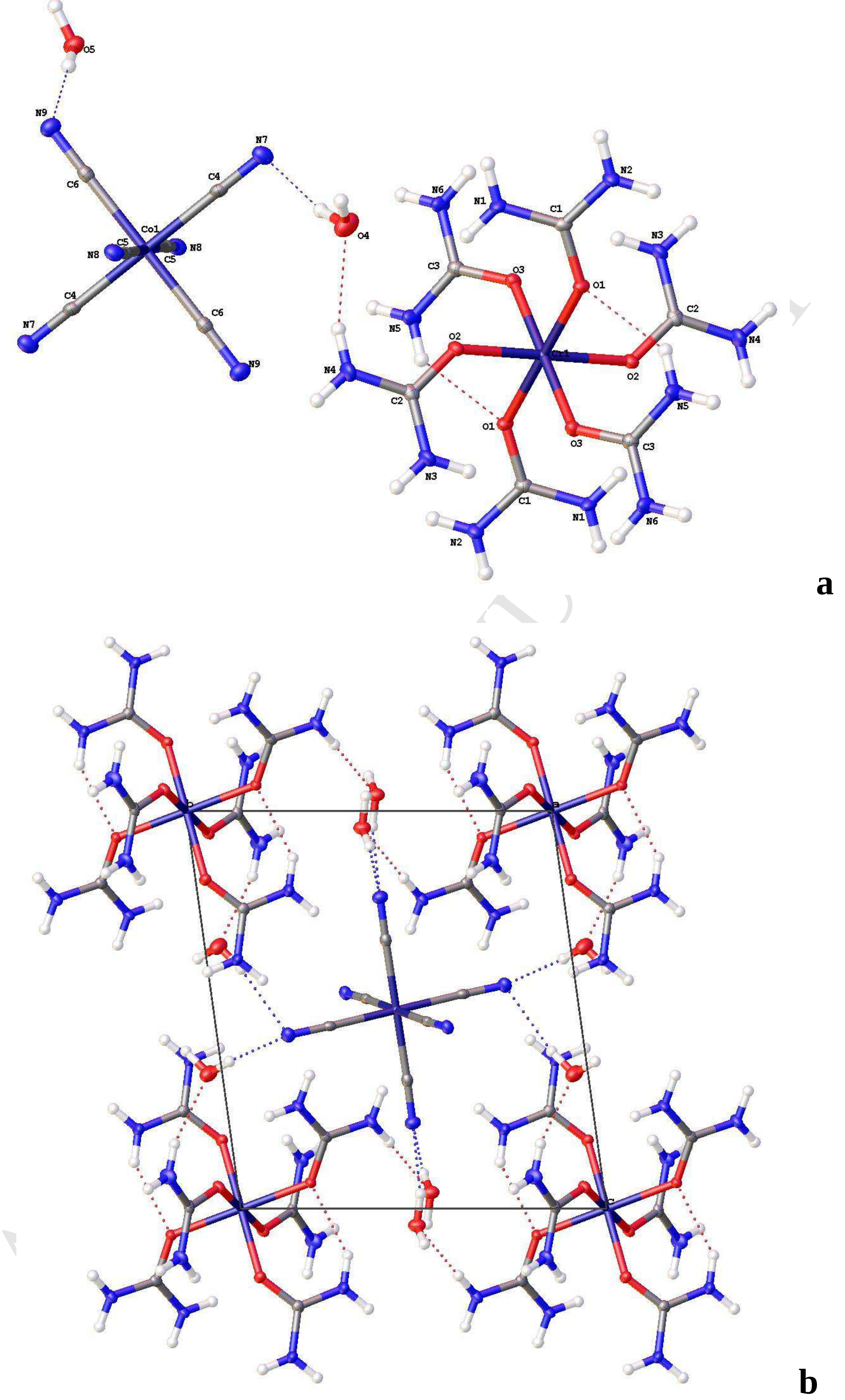

Figure 1. Structure of [Cr(*ur*)$_6$][Co(CN)$_6$]$^{\cdot}$4H$_2$O (**II**): crystallographically independent part (a); and packing of complex cations and anions in the structure (projection perpendicular to *a* axis) (b). The ellipsoids of thermal vibrations are plotted at a probability level of 50%. The hydrogen bonds are presented as dotted lines.

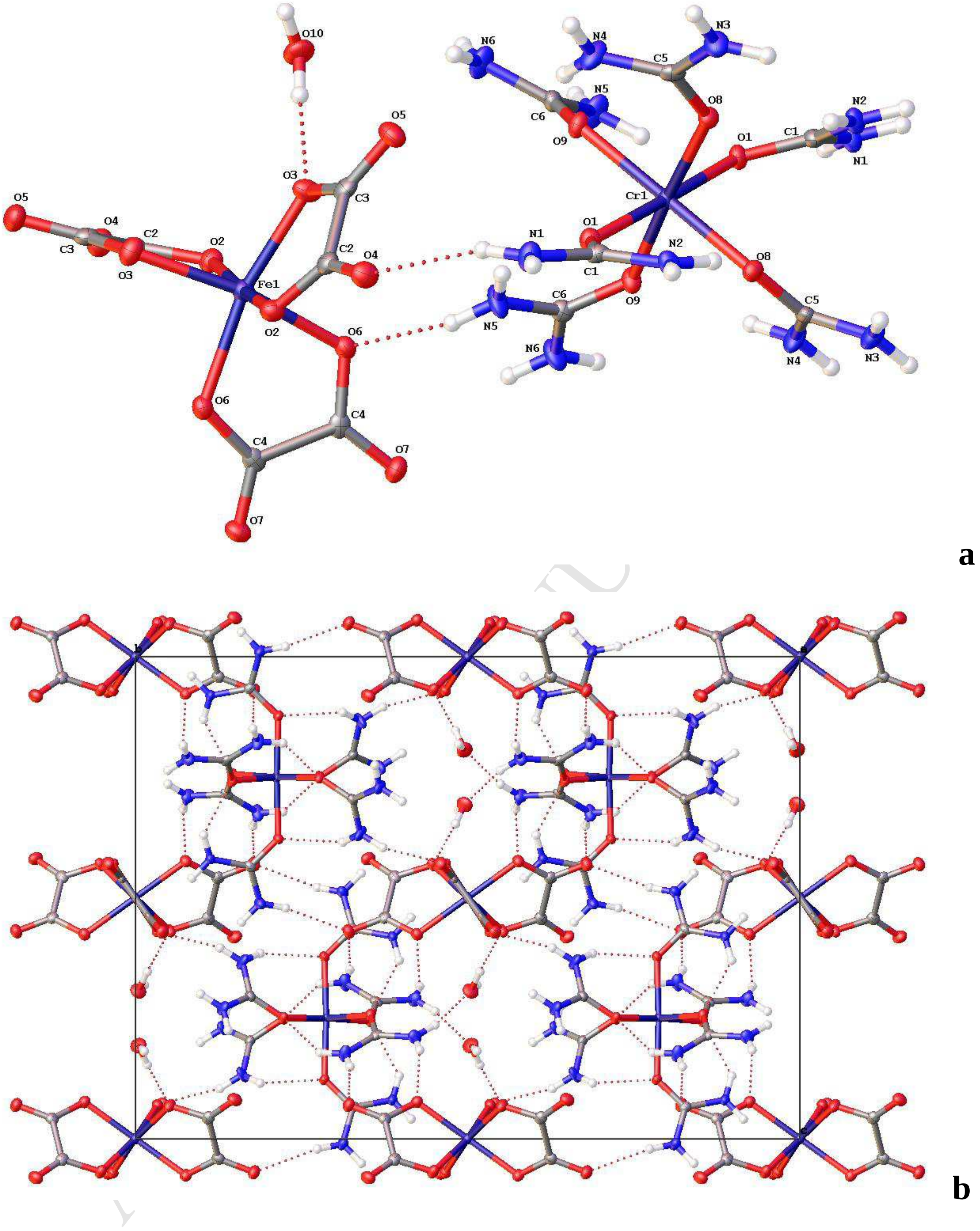

Figure 2. The structure of $[\mathrm{Cr}(\mathit{ur})_6][\mathrm{Fe}(\mathit{Ox})_3]\cdot 2\mathrm{H_2O}$ (**III**): crystallographically independent part (a); and packing of complex cations and anions in the structure (projection perpendicular to *a* axis) (b). The ellipsoids of thermal vibrations are plotted at a probability level of 50%. The hydrogen bonds are presented as dotted lines.

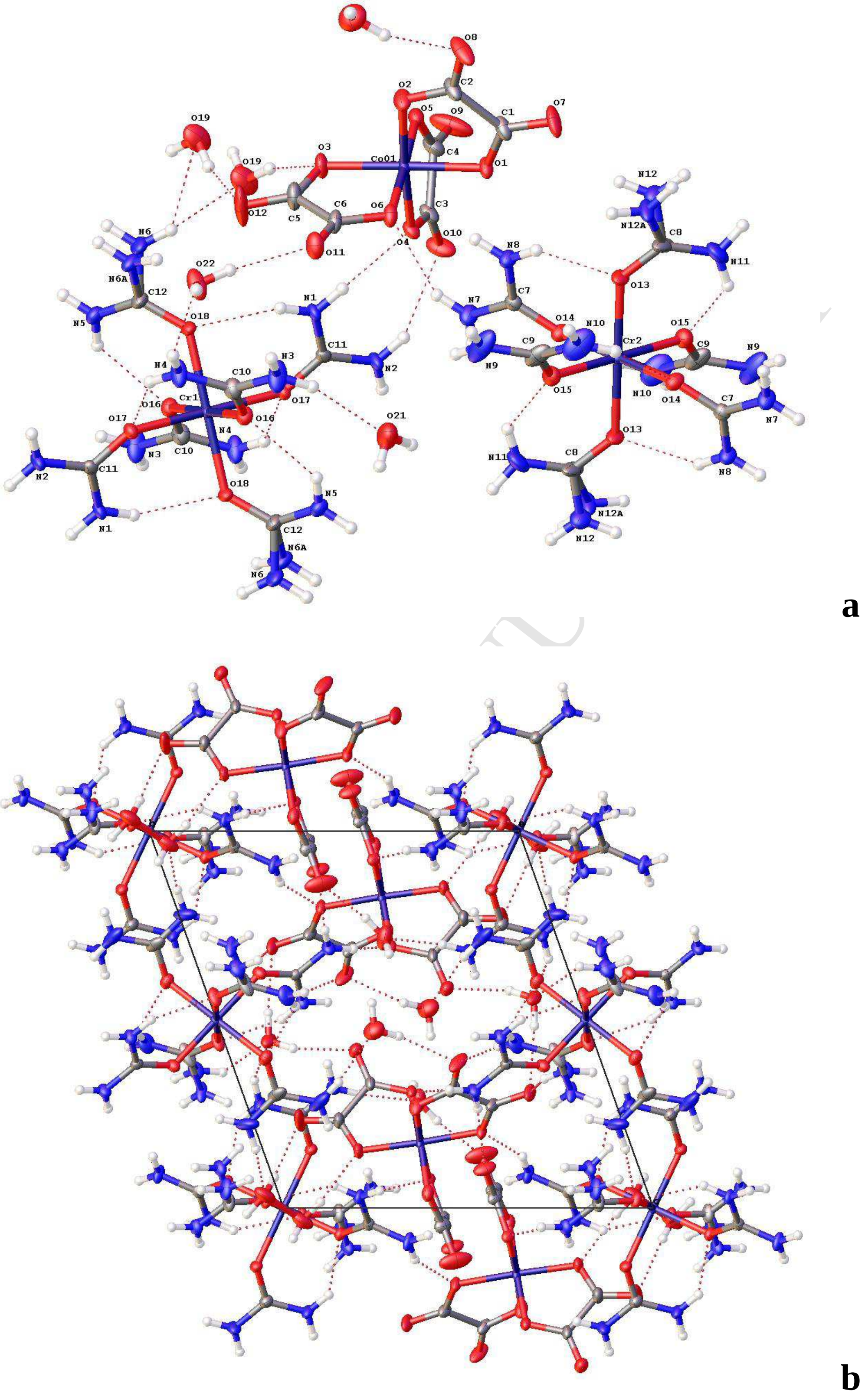

Figure 3. The structure of $[Cr(\mathit{ur})_6][Co(\mathit{Ox})_3]^{\cdot}3.5H_2O$ (**IV**): crystallographically independent part (a); and packing of complex cations and anions in the structure (projection perpendicular to *a* axis) (b). The ellipsoids of thermal vibrations are plotted at a probability level of 50%. The hydrogen bonds are presented as dotted lines.

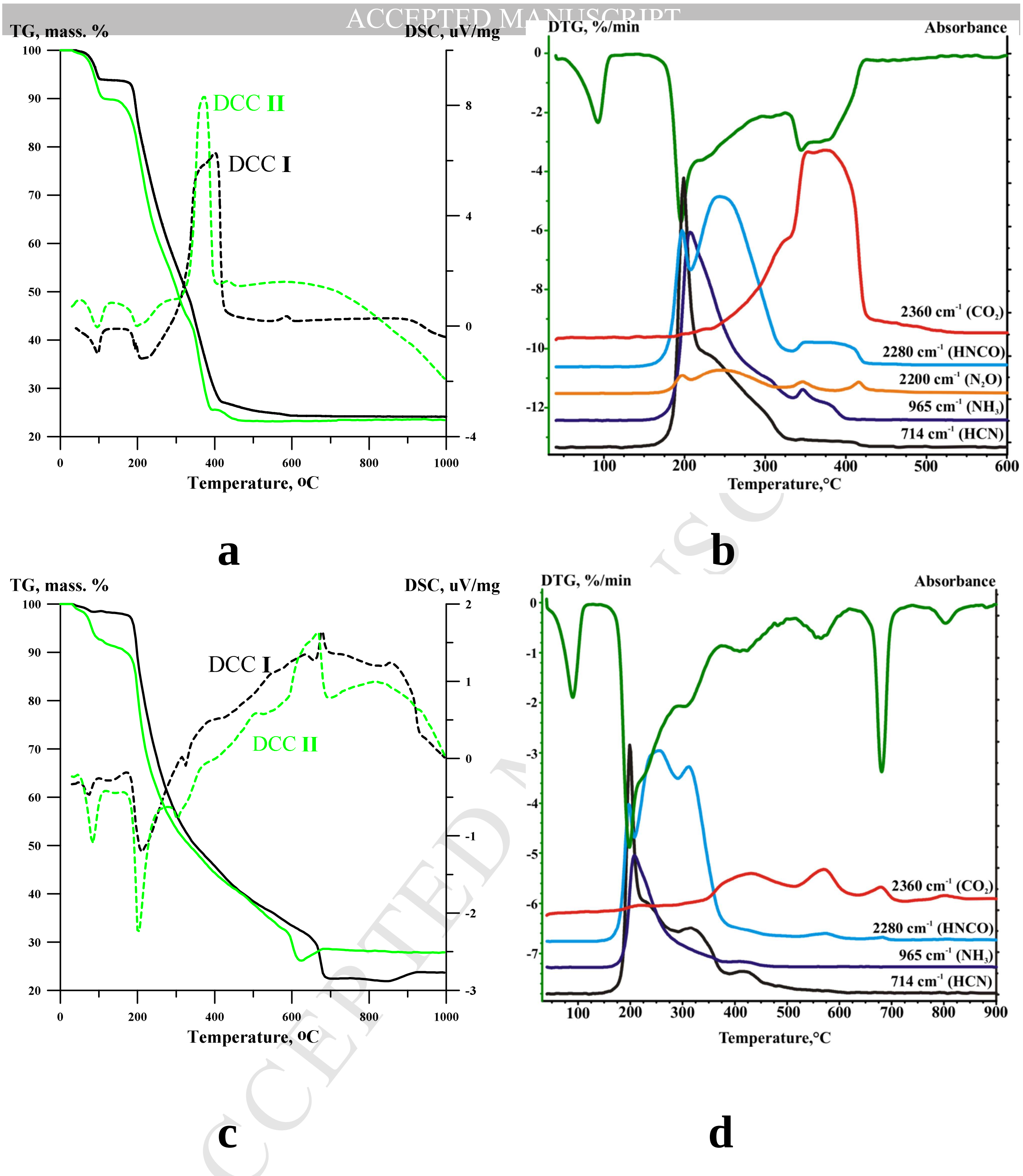

Figure 4. Thermal analysis of **I** and **II**. TG and DSC curves of **I** and **II**: a) in air; c) in argon. IR analysis of GPT for **I**: b) in air; d) in nitrogen.

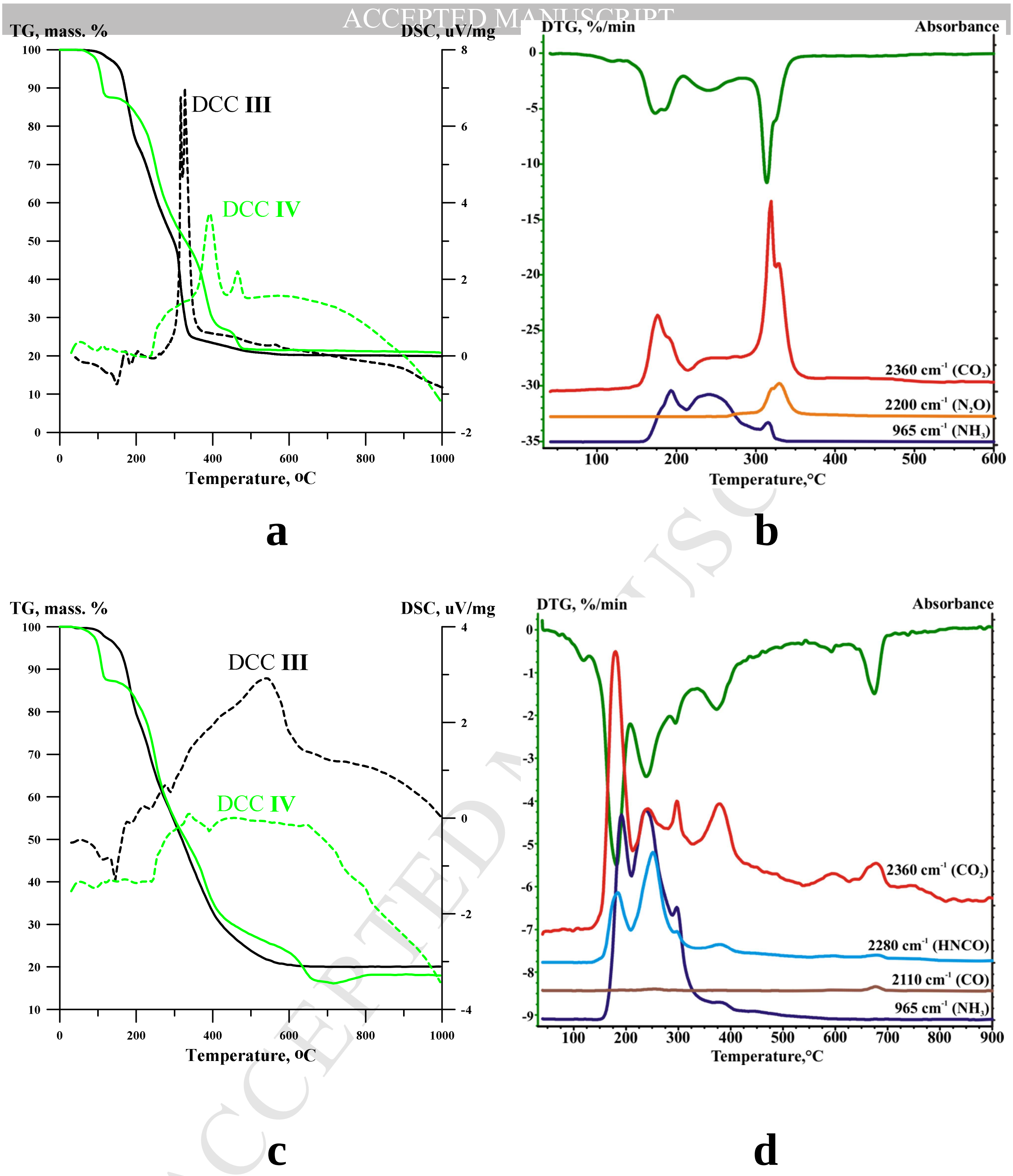

Figure 5. Thermal analysis of **III** and **IV**. TG and DSC curves of **III** and **IV**: a) in air; c) in argon. IR analysis of GPT for **III**: b) in air; d) in nitrogen.

The compounds $[Cr(CO(NH_2)_2)_6][ML_6]$ (M = Fe^{III}(**I**, **III**), Co^{III}(**II**, **IV**); L = $CN^{–}$(**I**, **II**), $1/2C_2O_4^{2–}$(**III**, **IV**) have been synthesized.

Their structures and thermal behavior have been studied. **I**, **II**, **IV** are triclinic, **III** is orthorhombic one.

The end solid products are spinels of type MCr_2O_4, gaseous products are HCN, NH_3, HNCO, N_2O, CO, CO_2, $CO(NH_2)_2$.